Particle Trapping for Acoustic Tweezers

Yanyan Yu, Weibao Qiu, Lei Sun

Department of Health Technology and Informatics, The Hong Kong Polytechnic University, Hong Kong, China

Email: htsunlei@inet.polyu.edu.hk

Abstract— **The optical tweezers has been found to have many biomedical applications in trapping macromolecules and cells. A recent theoretical study has shown that under appropriate conditions acoustic trapping is also possible [1]. Compared to the optical tweezers, the acoustic tweezers is more useful in light opaque media. In this paper, first we present the range where a particle can be trapped in single focused field along the axial direction from a 100MHz concave circular transducer on various sizes of particles. Secondly, we also proposed a multitrap model of acoustic tweezers which can trap 4 particles simultaneously. A 100MHz 2-D phased array with each line composed of 80 elements was used to generate and control the multiple-focus acoustic field. Both of the two fields generated by concave circular and phased array transducer were evaluated based on finite-element model. The radiation force was computed by the momentum transfer occurs between the mediums inside and outside the particle according to the law of conservation. The result demonstrates that the acoustic tweezers not only can manipulate larger particles, but also owns the feasibility of multitrap.**

I. INTRODUCTION

Since Ashkin reported the demonstration of optical tweezers in 1986[2], this powerful technology has progressed with its application in manipulating small particles with size from tens of nanometers to micrometers throughout both the biological and physical sciences. Compared to the optical tweezers, the acoustic tweezers with deeper penetration and lower energy is more useful in light opaque media. These advantages enhance the ability of acoustic tweezers in biological science.

Although theoretical study has shown that under appropriate conditions acoustic trapping of a particle is possible [1], the simulation is based on assumed Gaussian intensity distribution. In this paper, the intensity field was calculated by the radiation pattern generated with finite-element model instead of assumed Gaussian intensity distribution. The radiation force was computed by the momentum exchange occurs between the mediums inside and outside the particle according to the law of conservation. In order to manipulate microscopic particle precisely, the range in which small particle can be trapped by concave circular transducer was determined after motion analysis with considerations of radiation force and water velocity.

Furthermore, since the possibility of the acoustic tweezers has been demonstrated, various applications have required the simultaneous manipulation of many particles at the same time, such as sorting particles, placing them in creating patterns. A theoretical multitrap model of acoustic tweezers was established in this paper. The multiple-focus field was produced by 100MHz phased array transducer by computing array element amplitude and phase distribution. The radiation force was estimated in one of the 4 focus points along axial direction. The result shows that the acoustic tweezers has the potential of multitrap to produce a set of trapping points at desired positions.

II. METHODOLOGY

We propose to evaluate trapping range in consideration of the radiation force and water resistance. The analysis of radiation force was also applied in the multiple-focus field to demonstrate the potential of multitrap. In this section, we first introduce the theory of radiation force for the acoustic tweezers. Then we use finite-element model to generate single focused and multiple-focus acoustic field to estimate the radiation force.

A. The Theory of Acoustic tweezer and radiation Force

In physics, light can be considered as a series of propagating photons delivering momentum to the objects it interacts. In the concept of optical trapping, the momentum transferred from photons to the objects results in radiation force which can be decomposed into scattering and gradient force. Since acoustics wave has similar physics properties as optical wave, it transmits energy just like an electromagnetic wave or radiation. So the theory of calculating radiation force for the acoustic tweezers is analogous to the optical tweezers [3]. The axial radiation force can be estimated by integrating scattering and gradient force in the axial direction over a differential area where an incident ray interact the small particle. For simplicity, the particles are assumed to be spherical. In the Mie regime where particle size is larger than or close to the wavelength of incident ray, the complete formulations of radiation force can be described as follows [4]:

$$\mathrm{F_z} = \frac{1}{c_w}\int_s I\, ds = \frac{1}{c_w}\int_s I\, \mathrm{H}(\theta) d\theta \tag{1}$$

$$H(\theta) = \cos\theta_i \sin\theta \left\{ \cos(\theta_i - \theta) + R\cos(\theta_i + \theta) - \frac{T^2\left[\cos(\theta_i - 2\theta_r + \theta) + R\cos(\theta_i + \theta)\right]}{1 + R^2 + 2R\cos 2\theta_r} \right\} \tag{2}$$

$$R = \left| \frac{Z_2/\cos\alpha_2 - Z_1/\cos\alpha_1}{Z_2/\cos\alpha_2 + Z_1/\cos\alpha_1} \right|^2 \tag{3}$$

$$T = 1 - R\,. \tag{4}$$

where I is a surface integration of acoustic intensity. H(θ) indicates the fractional ratio of acoustic force. θ_i and θ_r are the incident and the refracted angles. θ is the angle between the

beam axis and a point where the incident ray impinges on the sphere. The quantities of R and T are fresnel reflection coefficient and transmission coefficient, respectively. Z_1 and Z_2 are the acoustic impedances of two mediums. α_1 and α_2 are the incident and transmitted angle.

In order to obtain intensity I, the amplitude of the acoustic pressure P will be introduced by the finite-element model. Each pressure point in the field was obtained by dividing the surface of the transducer into infinitesimal elements, each of which acts as a simple source [5]. The complex acoustic pressure at a point in the field is given by (5), and the intensity I is expressed by (6).

$$p(r,\theta,t) = \frac{j\rho c U_0}{\lambda}\int_s \frac{1}{r'} e^{j(\omega t - kr')} ds \tag{5}$$

$$I = \frac{P^2}{2\rho c} \tag{6}$$

where $j = \sqrt{-1}$, ρ and c are, respectively, the density of water and the speed of sound in water. λ is the wavelength. k is the wave number. s is the surface of the source. $U_0 e^{j\omega t}$ indicates the speed of piston moving. ω is the angular frequency. r is the distance from the origin of coordinates in the piston to the observation point, and r' is the distance from the source point to observation point. Then the intensity value for each point can be derived from the complex acoustic pressure here. Thus the axial radiation force can be obtained from a surface integration of acoustic intensity.

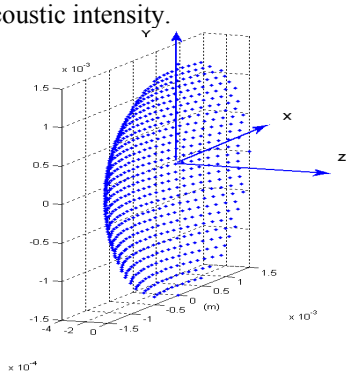

Fig. 1. A 100MHz single-element focused transducer with 3mm aperture and f#/1

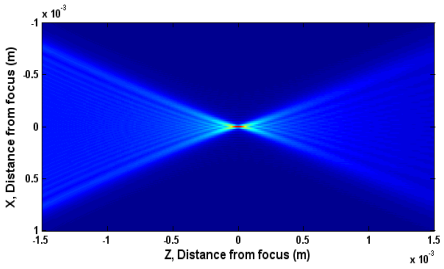

Fig. 2. Acoustic intensity field from a 100MHz single-element focused transducer with 3mm aperture and f#/1

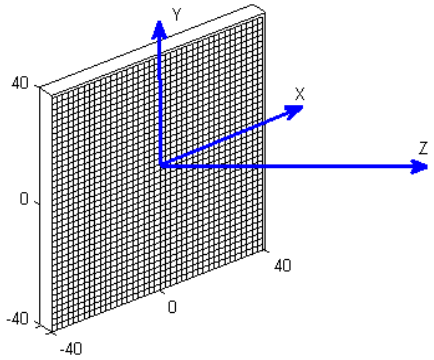

Fig. 3. Configuration of a phased array transducer used in the simulation with each line 80 elements.

B. Acoustic Field

In this section two types of acoustic field used for computing the trapping range and multitrap will be introduced respectively.

Firstly, the acoustic field for estimating trapping range was obtained using a single-element concave circular transducer with aperture of 3mm and f-number 1shown in Fig. 1. Its center frequency is assumed to be 100 KHz. The speed of sound in water and the density of the water are 1500 m/s and 1000 Kg/m^3. The impedance of water is 1.5MRayls. Input acoustic power is 1mW. According to the parameters given above, the intensity field for single focused concave transducer was obtained and shown in Fig. 2 based on (5) and (6).

Secondly, to demonstrate the potential of the acoustic multitrap, a 100MHz phased array with each line 80 elements (Fig. 3) was used to generate and control the multiple-focus acoustic field. Each element was composed of 121 sub-elements with a side length of one tenth the size of wavelength. Simulation results were obtained by the pseudoinverse approach. In order to produce desired control points in the acoustic field, a discretizing matrix propagation operator generated by the Rayleigh-Sommerfeld was applied in our simulation [6]:

$$H(m,n) = \frac{j\rho ck}{2\pi}\int_{S'_n} \frac{e^{-jk|r_m - r'_n|}}{|r_m - r'_n|} dS'_n \tag{7}$$

$$\hat{u}_w = WH^{*t}(HWH^{*t})^{-1}P \tag{8}$$

where H is the forward propagation operator with m*n elements. S' is the surface of the nth element of the array. r_m and r'_n represent the coordinates of the mth point in the field and the nth element of the array. $\hat{u}_w$ is weighted minimum norm solution to the complex excitation vector of the array elements. The vector P denotes the complex pressure at each of the control points in the field. W is an N x N real, positive definite weighting matrix.

The idea is that the complex excitation vector of the array elements (8) is evaluated by inverting the propagation matrix operator (7) using the generalized inverse approach. In order to increase the array excitation efficiency, an iterative weighting

algorithm was used based on (8). Then the complex excitation vector is solved through (8). Thus, intensity field can be obtained by combining complex excitation and (5) and (6). Fig. 4 shows the plot of the array excitation efficiency against the number of iteration we used. The results with 4 focus points in X-Y and X-Z plane are shown in Fig. 5. For the aim of enhancing the function of multitrap, we can create different patterns of multiple-focus intensity field by solving (8) with different complex pressure at each of the control points. Fig. 6 shows acoustic intensity field for 12 focus points in 2D and 3D forms, respectively.

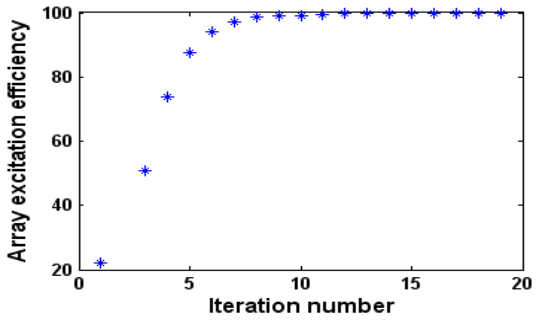

Fig. 4. Array excitation efficiency versus iteration number of iterative weighting algorithm.

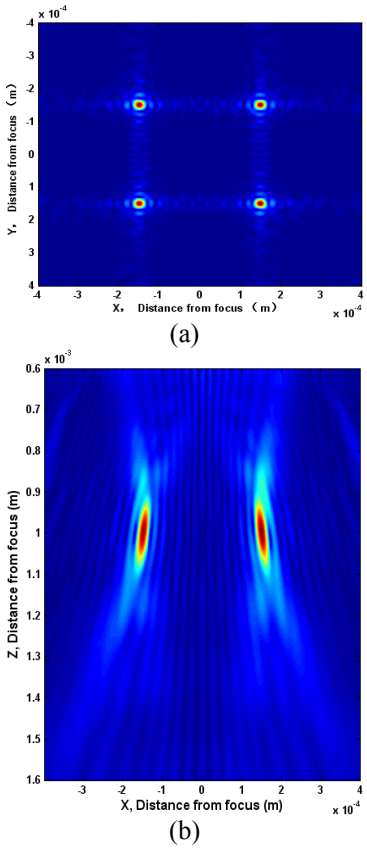

(a)

(b)

Fig. 5. Acoustic intensity field for 4 focus points. (a) Acoustic intensity field in X-Y plane (b) Acoustic intensity field in X-Z plane

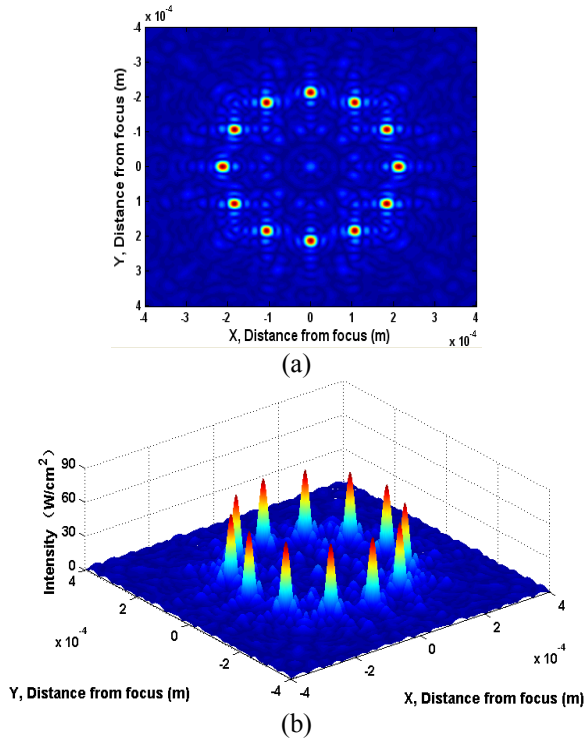

(a)

(b)

Fig. 6. Acoustic intensity field for 12 focus points. (a) 2D acoustic intensity field for 12focus points in X-Y plane. (b) 3D acoustic intensity field for 12focus points in X-Y plane.

III. RESULTS AND DISCUSSION

For the aim of evaluating the trapping range and demonstrating the feasibility of multitrap, the radiation force with particles along axis direction is a critical issue.

Here the axial radiation force produced by a 100MHz single-element focused transducer was calculated using (1)~(6). Besides the parameters mentioned above, other parameters include the sound speed in sphere 1450m/s, impedances of sphere and water are 1.4MRayls and 1.5MRayls, respectively. The result of radiation force for a sphere with diameter of 120μm along the beam axis was shown in Fig. 7. The negative force is drawing force, while the positive force is propelling force. It can be seen that the negative force is in between 5μm to 250μm to focus point. Besides the radiation force, the resistance due to viscosity of water was taken into consideration as $F = -6\pi\mu Rv$, where μ is the viscosity coefficient of water at 25 °C with quantity $8.9*10^{-4}$Pa·s, R and v indicate the radius and the velocity of the sphere, respectively [7]. If the sphere with initial speed 0 is in the position beyond 250μm, it will be pushed and never come back. The trapping range in which the sphere can be trapped to the balance position was calculated in the initial location where is in the end of negative points. The range where a particle can be trapped was determined after the analysis according to Newton's second law of motion. For comparison, the displacement trajectory of four spheres along the axial direction with various diameters was displayed in Fig.8. It is noted that particles can be captured quickly within 0.1 second and the larger particle has the longer time to get balance. Table I summarizes the axial trapping regions and

balance position, respectively. It demonstrates that the acoustic trapping has the ability to quickly capture large particles in the range of tens of to hundreds of microns. It also shows that the range increases as the size of the particles increased.

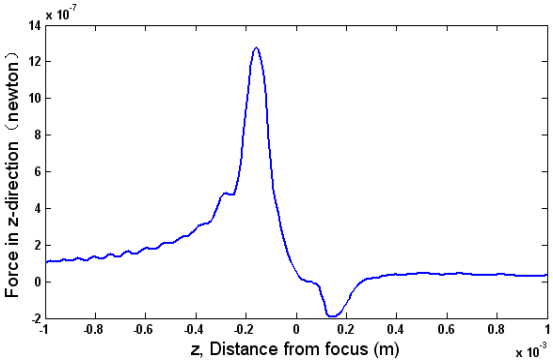

Fig. 7. Radiation force along the beam axis

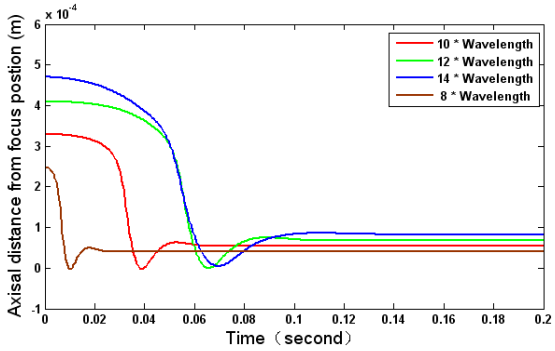

Fig. 8. Displacement trajectory of the particles along the axial direction with various diameters

TABEL I

Trapping region along the axial and lateral direction.

Particle diameter（μm）	Axial trapping range (μm)	Force balanced position(μm)
120	253.3	82.81
150	332	68.8
180	408.28	54.91
210	464.524	41.41

To demonstrate the feasibility of multitrap, the acoustic intensity field with multiple-focus points shown in Fig. 5 has been created by a 100MHz phased array transducer with parameters as mentioned above. Then the radiation force can be evaluated based on the multiple-focus point field combining (1) ~ (6). The radiation force of the sphere with diameter of 120μm along the beam axis in multiple-focus field is shown in Fig. 9. It can be seen that the negative force exists in between two positive force areas. This means that the particle can be trapped.

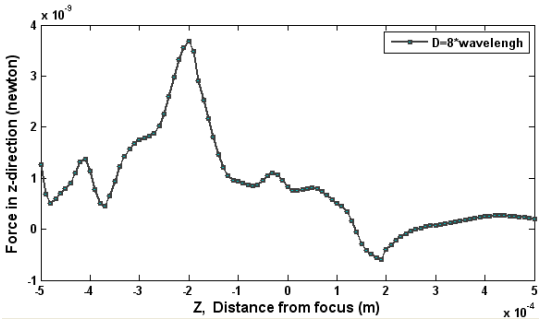

Fig. 9. Shows the radiation force of a fat sphere with diameter of 120 micron along the one of the four beam axises.

IV. CONCLUSION

The results in this paper confirm that acoustic trapping is feasible using the intensity field calculated from a single focused transducer and multiple-focus phased array transducer. For single focused field the region where the particles can be trapped along the axial direction was determined. It demonstrates that the acoustic trapping has the ability to quickly capture large particles in the range of tens of to hundreds of microns. It also shows that the range increases as the increased size of the particles.

ACKNOWLEDGEMENT

The financial support from the Hong Kong Research Grant Council (RGC) General Research Fund (GRF) (PolyU 5028/10P), and The Hong Kong Polytechnic University (G-YH67) are gratefully acknowledged.

REFERENCES

[1] J . Lee and K. K. Shung, “Radiation forces exerted on arbitrarily located sphere by acoustic tweezer,” J. Acoust. Soc. Am., vol. 120, No. 2, pp. 1084-1094, 2006.

[2] A. Ashkin, J. M. Dziedzic, J. E. Bjorkholm, and S. Chu, “Observation of a single-beam gradient force optical trap for dielectric particles,” Opt. Lett. vol.11, No. 5, pp. 288-290,1986.

[3] A. Ashkin, “Forces of a single-beam gradient laser trap on a dielectric sphere in the ray optics regime”, Biophys. J., vol. 61, issue 2, pp. 569–582, February 1992.

[4] J . Lee and K. K. Shung, “A theoretical study of the feasibility of acoustical tweezers: ray acoustics approach,” J Acoust. Soc. Am. Vol. 117, No. 5, pp. 3273-3280, 2005.

[5] L. E. Kinsler, A. R. Frey, A. B. Coppens and J. V. Sanders, “Fundamentals of Acoustics,” New York, 2000, pp.179.

[6] E. Ebbini and C. Cain, "Multiple-focus ultrasound phased-array pattern synthesis: optimal driving-signal distributions for hyperthermia," IEEE Trans. Ultrasonics, Ferroelectrics and Frequency Control, vol. 36, No. 5, pp. 540-548, 1989.

[7] L.D.Landau and E.M. Lifshitz, Fluid Mechanics, 2nd ed., Pergamon, New York, 1987, pp. 61&252.